The impact of smart completions on optimal well trajectories

Maas, T. R.; Bouts, M. N.; Joosten, G. J.P.; Jansen, J. D.

Citation (APA)
Maas, T. R., Bouts, M. N., Joosten, G. J. P., & Jansen, J. D. (2017). The impact of smart completions on optimal well trajectories. In *Society of Petroleum Engineers - SPE Abu Dhabi International Petroleum Exhibition and Conference 2017* (Vol. 2017-January). Article SPE-188368-MS Society of Petroleum Engineers. https://doi.org/10.2118/188368-MS

Important note
To cite this publication, please use the final published version (if applicable).
Please check the document version above.

SPE-188368-MS

The Impact of Smart Completions on Optimal Well Trajectories

T. R. Maas, Shell, Delft University of Technology; M. N. Bouts; G. J. P. Joosten, Shell Global Solutions Int.; J. D. Jansen, Delft University of Technology

Abstract

When new wells are planned, typically the same trajectory is used for assessing the effectiveness of conventional wells and wells with smart completions. This study demonstrates that the economically optimized trajectory for smart and conventional wells can be very different. Two new well trajectory optimization algorithms were developed using Stochastic Pattern Search (SPS) principles. In both algorithms, random perturbations are made starting from an initial well trajectory, which are sent to a reservoir simulator. Thereafter the perturbation with the highest Net Present Value (NPV) is selected. New perturbations of the selected well trajectory are made and simulated to, again, select the highest NPV. This process is repeated until a certain stopping criterion is met. The two methods differ in the selection of the perturbations used to initiate the new iteration and have a slightly different computational performance. To demonstrate the difference between the optimal well trajectory of a well with a conventional and a smart completion, both the SPS1 and SPS2 method were evaluated using a realistic, but slightly simplified reservoir model. Both methods were able to optimize the trajectory for both conventional and smart completions. The SPS1 method quickly converged to a local optimum, whilst the SPS2 method was able to determine a trajectory with a significantly higher NPV for both the conventional and smart wells. Moreover, the optimal well trajectory with the smart completion, as found by the SPS2 algorithm, had an NPV that was 40% higher than the smart well with the trajectory which was optimal for the conventional completion. Following the above, it can be concluded that when smart completions are assessed, well trajectory (re)optimization can have a very significant value impact and may be crucial in evaluating the full potential of the completion. Furthermore, it was shown that, for the investigated case, the SPS2 procedure is a good method for well trajectory optimization in a three-dimensional reservoir and, although more testing is needed, it is believed that it has potential to work with any type of completion.

Introduction

Smart wells, sometimes referred to as intelligent wells, have become an increasingly common well completion option to maximize the economic value of a reservoir. In general, smart well completions have some form of downhole inflow control. There are three main types of inflow control completions: passive Inflow Control Devices (ICDs), active Inflow Control Valves (ICVs) and Autonomous Inflow Control

Devices (AICDs). An ICD is a preset flow restriction that creates a certain pressure drop to control the flow from the reservoir into the well. By equalizing the inflow along the well, ICDs are mainly used to overcome sweep efficiency issues caused by differences in reservoir permeability and by the heel-to-toe pressure drop in horizontal wells. An ICV is a valve that can be controlled from the surface. It restricts the flow from the reservoir into the well by partially or fully closing the valve. Initially designed to allow for commingled production of multiple reservoirs, ICVs are now also being used to mitigate inflow or injection imbalance and to optimize well and field management (Al-Khelaiwi 2013). An AICD is a device that can self-adjust the closing of the valve depending on the viscosity of the fluid (mixture) that passes through the device. It has the ability to delay the breakthrough of water or gas using an effect based on their viscosity being lower than that of oil. Similar to the AICD is the Autonomous Inflow Control Valve (AICV). The advantage of an AICV over an AICD is that it can shut off unwanted gas and water production completely. The AICV is also reversible, which means that a closed valve can autonomously open itself once it detects oil again.

Over the years, several studies have assessed the benefits of smart completions. They have combined geological and/or economic uncertainty with different smart well completion configurations and several ICV control optimization strategies (Van Essen et al. 2010, Grebenkin 2013, Addiego-Guevara et al. 2008, Schiozer and Silva 2009, Pinto et al. 2012). Although it has been recognized that the choice of an optimal well trajectory is crucial to maximize the economic value of a reservoir, no studies have been found on well trajectory optimization for smart wells. The objective of this paper is to demonstrate that the optimal well trajectory for a well with a smart completion can be different compared to the optimal trajectory of a well with a conventional completion.

Literature review

A wide variety of optimization methods (with wildly varying names and acronyms) have been used for model-based hydrocarbon recovery optimization. These can be classified into two main groups: gradient-based and gradient-free methods. Both can further be divided into deterministic and stochastic techniques. Moreover, a distinction can be made between methods that aim at optimizing well controls (production rates, well pressures or ICV settings) for a given well configuration, and those that aim at optimizing the configuration itself (i.e. the well locations and/or trajectories).

The main advantage of gradient-based over gradient-free approaches is their computational efficiency, especially for deterministic optimization problems. Gradient-based methods do, however, have some shortcomings. Most model-based hydrocarbon recovery optimization problems are non-convex. As a result, they generally contain multiple optima in which the local search of the gradient approach can get trapped. Furthermore, the optimization surface can be very rough, which can result in discontinuous gradients (Echeverría Ciaurri et al. 2011a).

Optimization of well controls in 'smart wells' for a given configuration can be done with a short-term, operational focus, see, e.g., Gai (2001) and Naus et al. (2006), or by considering the full operational life-cycle (often referred to as well control optimization), see, e.g., Brouwer and Jansen (2004), Sarma et al. (2005), Van Essen et al. (2010), and Fonseca et al. (2015). All these life cycle optimization methods are gradient-based and use the adjoint-method to compute the gradient which is computationally very efficient; see Jansen (2011) for an overview. However, unlike gradient-free or approximate gradient methods, which treat the reservoir simulator as a black box, the adjoint method has the disadvantage that it requires access and detailed knowledge of the simulation source code to be implemented.

Stochastic gradient-based methods (i.e., approximate gradient methods) for life-cycle optimization are, e.g., the Simplex gradient (Do and Reynolds 2013), and the Ensemble Based Optimization (EnOpt) method (Chen 2008, Chen and Oliver 2010) with varieties such as the Stochastic Simplex Approximate Gradient (StoSAG) method (Fonseca et al. 2017). Another alternative to the use of the adjoint method is through streamline-based optimization; see, e.g., Alhuthali et al. (2009).

Many well location and trajectory optimization studies, including the earliest ones, used Genetic Algorithms (GAs – a stochastic gradient-free method); see, e.g., Güyagüler et al. (2002), Yeten et al. (2003), Güyagüler and Horne (2004), Emerick et al. (2009), and Lee et al. (2009). Other stochastic approaches for well location optimization that have been reported in the literature include the Simultaneous Perturbation Stochastic Approximation (SPSA) and Simulated Annealing (SA) methods (Bangerth et al. 2006), the Covariance Matrix Adaptation Evolutionary Strategy (CMA-ES) (Bouzarkouna et al. 2011), Particle Swarm Optimization (PSO) (Owunalu and Durlofsky, 2010), and Improved Harmony Search (IHS) (Afshari et al. 2011).

Deterministic gradient-based approaches that have been used for well location and trajectory optimization are the Finite Difference Gradient (FDG) method (Bangerth et al. 2006) and the, computationally much more efficient, adjoint-based method (Zandvliet et al. 2008, Sarma and Chen 2008, Vlemmix et al. 2009, Zhang et al. 2010, Loomba 2015).

Several truly gradient-free stochastic methods have also been applied, primarily for well location optimization. These include the Generalized Pattern Search (GPS), Mesh Adaptive Direct Search (MADS) and Hooke-Jeeves Direct Search (HJDS) methods and their varieties; see Echeverría Ciaurri et al. (2011a, 2011b). Moreover, some optimization methods combine gradient and gradient-free techniques with deterministic and stochastic features; see, e.g., the Simultaneous Perturbation and Multivariate Interpolation (SPMI) method (Gao et al. 2014).

Recently, several papers have been published addressing the combined optimization of well locations and well rates or pressures, using a variety of methods, see, e.g., Isebor et al. (2014), Forouzanfar and Reynolds (2014), Forouzanfar et al. (2016), and Humphries and Haynes (2015). Other studies focus on smart wells from a more operational perspective addressing different optimization strategies (Sampaio et al. 2012) or model-free closed-loop methods (Jansen et al. 2002, Dilib et al. 2015), or elaborate on the choice between ICDs, ICVs or AICDs (Al-Khelaiwi et al. 2010).

Trajectory Description and Optimization Strategy

Many well trajectory optimization methods only vary the heel and toe location of the well, resulting in a straight well path; see, e.g., Emerick et al. (2009). The main advantage of this method is that it results in a relatively small dimensional optimization problem, involving six dimensions [heel (x_1; y_1; z_1) and toe (x_2; y_2; z_2)]. The disadvantage of the method is that the well does not have the freedom to change its straight shape and therefore cannot follow the contours of a specific layer. This can result in a too simplistic and suboptimal well trajectory. Fig. 1 shows a two-dimensional (2D) example of a well trajectory were only the heel and toe locations are varied.

A single-well trajectory optimization method for 3D reservoirs developed by Vlemmix et al. (2009) allows the well to move more freely through the reservoir by dividing the well into several subsections. Fig. 2 shows an example of this. The strategy makes use of the adjoint-based method and was shown to be successful for well trajectory optimization in a thin oil rim example. Since the reservoir simulator used in the present research had no built-in adjoint functionality, nor was there access to the source code, this method could not be used. As a result, a new single-well trajectory optimizer in 3D had to be developed. Furthermore, the adjoint-based method has the downside that it can easily get stuck in a local optimum. The newly developed method also sought to overcome this issue.
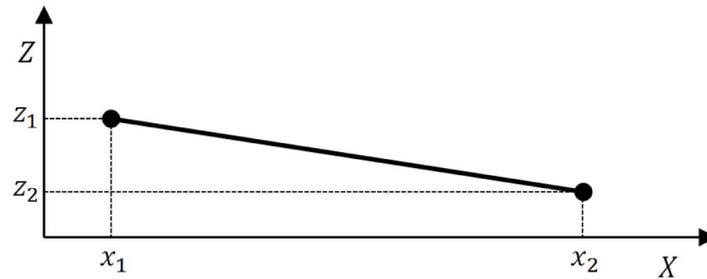
Figure 1—A 2D, x-z, view of a well path with only heel and toe location.

The description (parametrization) of the well trajectory is critical to the optimization scheme. In this research, just as in Vlemmix et al. (2009), the well is divided into N subsections. Every well section is described by its length (L), inclination (θ) and azimuth (φ). To determine where the well starts, the x, y and z location of first node of the first well section are defined as B_x, B_y and B_z. This results in the number of dimensions of the optimization problem being equal to $3(N + 1)$. When the well is, for example, divided into 10 sections (i.e., $N = 10$) this results in an optimization problem with 33 dimensions. Fig. 2 and Fig. 3 show a 2D and 3D example of a well trajectory respectively. The reason that the well sections are described in spherical coordinates instead of Cartesian coordinates is discussed in Section 3.2.1.
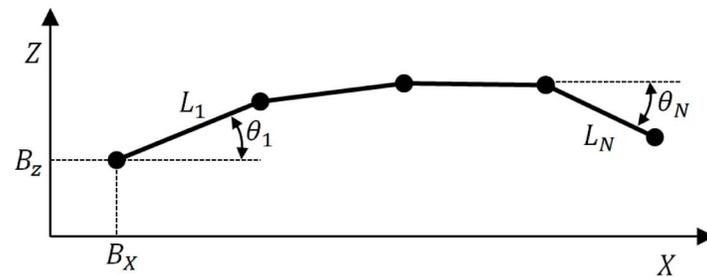
Figure 2—A 2D, x-z, view of an example well trajectory divided in N sections.

A commercial reservoir simulator (Petex 2015) was used in this research. The simulator was used as a black box. There were a maximum of 10 concurrent simulation runs possible on the available machine. In other words there were only 10 evaluation of the objective function possible per iteration. Gradient-free methods like GAs, PSOs and IHS, which generally require a population size that is equal to or several times greater than the number of dimensions of the problem, were for this reason not evaluated. If, for example, a population size that is equal to the number of dimensions would be chosen, the well could only be divided into a maximum of two sections, which would severely restrict the trajectory freedom of the well.

Figure 3—A 3D view of the first well section of an example well trajectory.

The EnOpt method, as developed by Chen (2008), was the first approximate gradient method that was evaluated in our study. Although SPSA has shown to achieve good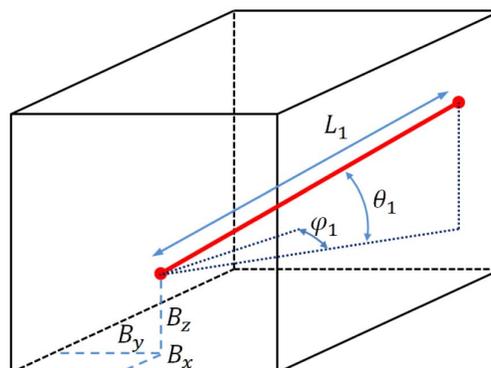 results in well placement optimization for simple 2D reservoirs (Bangerth et al. 2006), the EnOpt method was considered more appropriate because of the following. It is important in approximate gradient techniques that the sample size (i.e. the number of evaluations of the objective function per iteration) is big enough to achieve convergence of the algorithm and good quality solutions. The general consensus is that a large sample size relative to the dimensions of the problem produces higher quality gradients and better results. Because SPSA requires twice as many objective function evaluations for the same number of samples per iteration as EnOpt, the EnOpt method was evaluated instead of SPSA. It must be noted that the maximum number of concurrent runs that are possible on a machine do not limit the number of samples per iteration, but only increases the computation time. A trade-off has been made between optimization speed and quality by setting the amount of samples that can be used per iteration equal to the maximum number of possible concurrent runs.

The EnOpt method was tested on simple box models. Details about the implementation of the EnOpt method can be found in Appendix D of Maas (2016). To achieve a proper gradient out of the 10 ensemble members, relatively small perturbations and a small step size were needed. Although the algorithm was able to find an optimum, random testing of well trajectories and the analysis of the objective functions of the ensemble members showed that there were higher optima in the same space. By analyzing the objective function data of the ensemble members, it was found that the stochastic element of the EnOpt method could potentially be used without approximating a gradient. For this reason, a Stochastic Pattern Search (SPS) method (Hart 2001) was evaluated.

Stochastic Pattern Search

The SPS optimization method is an example of a Pattern Search method, which is a subset of Direct Search methods. In Hooke and Jeeves (1961), Direct Search is described as: "the sequential examination of trial solutions involving comparison of each trial solution with the "best" obtained up to that time together with a strategy for determining (as a function of earlier results) what the next trial solution will be". How to determine the parameters to obtain these trial solutions and subsequently move forward from these solutions determines the type of Direct Search method. Generally speaking "Pattern Search methods are characterized by a series of exploratory moves that consider the behavior of the objective function at a pattern of points" (Hart 2001, Torczon 1997). In the SPS method the exploratory moves are selected randomly.

Implementation

To create a stochastic pattern of exploratory moves, the well trajectories need to be perturbed randomly. This is done by defining the trajectory as a control vector comprised of the following variables:

$$\mathbf{u} = \begin{bmatrix} B_x B_y B_z L_1 \theta_1 \varphi_1 \cdots L_N \theta_N \varphi_N \end{bmatrix}^T \tag{1}$$

The control vector is sent to a reservoir simulator, which transforms it into a well trajectory. The starting point from where the perturbations are created during every iteration is the control vector $\mathbf{u}^\ell$. During the first iteration $\mathbf{u}^\ell$ is the initial well trajectory. Perturbations of $\mathbf{u}^\ell$ are created as

$$\mathbf{u}_i = \mathbf{u}^\ell + \mathbf{C}\mathbf{z}_i \tag{2}$$

where $\mathbf{u}_i$ is the perturbation of $\mathbf{u}^\ell$ and is defined as an ensemble member. The counter of the ensemble members is denoted with i. The counter of the iteration is ℓ. $\mathbf{C}$ is a diagonal matrix in which the degree of perturbation per control variable is specified. The matrix is specified by the user and can differ per reservoir. If, for example, the reservoir is relatively thick, larger values in the entries of $\mathbf{C}$ that correspond to B_z and

θ can be taken than when dealing with a thin reservoir. The **C** matrix is multiplied by a vector **z** whose variables are drawn from an univariate Gaussian distribution. Although the use of distributions other than Gaussian could be viable, they were not investigated in this paper. The algorithm can be set up such that the runs are reproducible by using the same random seed. In this research a seed is used that is based on the value returned by the system clock of the machine to ensure a different value for each random sample.

Two different algorithms were developed: Stochastic Pattern Search 1 and 2 (SPS1 and SPS2). The SPS1 method evaluates the objective functions for both $\mathbf{u}^\ell$ and $\mathbf{u}_i$. The control vector with the highest objective function becomes $\mathbf{u}^{\ell+1}$. The SPS2 method only evaluates the values for $\mathbf{u}_i$ which implies that the new iterate $\mathbf{u}^{\ell+1}$ cannot be equal to the previous iterate $\mathbf{u}^\ell$.

Both algorithms were subjected to the same test function, namely the Rastrigrin function. This function, as described in Molga and Smutnicki (2005), has a global minimum and numerous local minima and is commonly used to test the performance of minimization procedures. Because the objective function used in this paper is the net present value (NPV), the Rastrigin function was rewritten to a maximization function, as expressed in Equation 16. In Fig. 4 the results of the SPS1 and SPS2 algorithm are displayed when subjected to Equation 16. In both methods, the same **C** matrix, where both non-zero values where 0.2, and the same number of ensemble members and iterations were used. The blue marker [-1, -0.5] in the plots shows the starting point ($\mathbf{u}^\ell_1$) of the algorithms. The red marker, corresponding to the point [0, 0], represents the location of the global maximum. As can be seen in the left plot, the SPS1 methods was able find the location of a local maximum, but the algorithm got stuck in the that point. The advantage of the method is that it has a high probability of convergence compared to SPS2.

The right plot shows how the SPS2 algorithm performed on the test function. Although it is theoretically impossible for the algorithm to converge, the method was able to (approximately) locate both the global maximum and several local maxima. To ensure that the SPS2 method does not get stuck in local optima, the number of ensemble members should be limited. When a small number of ensemble members is used, the sampling is done less dense, which increases the probability of entering a neighboring domain of attraction. The downside is that in cases where the evaluation of the objective function takes a considerable amount of time, it can be argued that using more evaluations of the objective function increases the chance to find an optimum. When the SPS2 method is used for an optimization problem, a trade-off between these two features is needed by tuning the number of ensemble members used. In this study this was done by trial-and error. In addition to this, tuning of matrix **C** is needed.
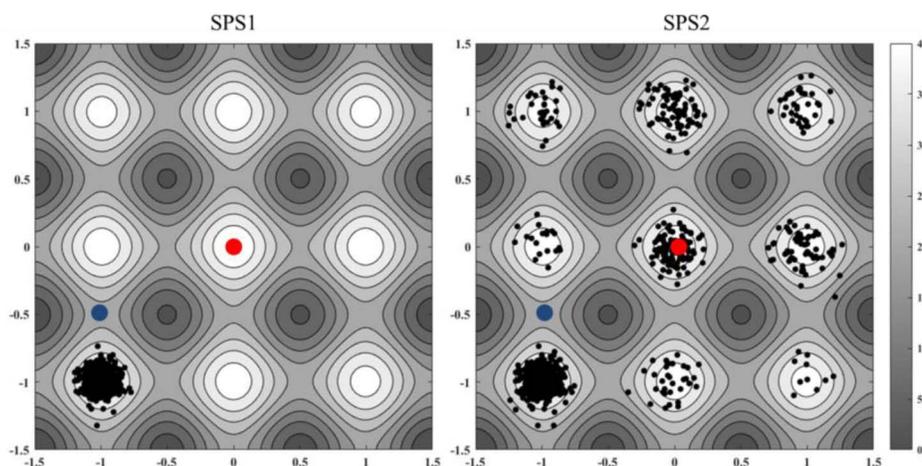
Figure 4—The figures shows two contour plots of the Rastrigin function. The left plot shows how the SPS1 method works on the Rastrigin function as seen in Equation 16. The right image shows how SPS2 reacts to the same function. The blue markers in the images show the starting point of the algorithm on [-1, -0.5]. The red markers show the location of the global optimum on [0, 0]. The black dots in both plots show the location of u^ℓ during all iterations.

Control Vector Constraints

To evaluate the objective function corresponding to the control vector a complete reservoir simulation is carried out. Every well that is sent to the reservoir simulator has to meet two conditions. The first is that the well has to stay within the dogleg severity (DLS) limit. The second is that the well has to lie within the reservoir. If a well that is constructed by the algorithm does not honor these two constraints, the algorithm discards the well and generates a new random well until it meets the two conditions. Both these evaluations require much less cpu time than the full reservoir simulation.

Dogleg Severity

To ensure that every modelled well trajectory is drillable and can be completed at least below the kick-off point, it has to stay within the DLS limit (Vlemmix et al, 2009). The dogleg angle (β) describes the overall angle change of the curve between two consecutive directional survey points. Depending on the completion type of the well, a maximum DLS [°/30m] can be chosen as an input variable for the optimization algorithm.

The control variables, except for the first three which describe the location of the first node, are described in spherical coordinates instead of Cartesian ones. This is done to increase the likelihood that the algorithm creates wells that stay within the DLS limit whilst exploring a large section of the reservoir. If Cartesian coordinates of the nodes are perturbed, they change independently from each other, increasing the chance of hitting the DLS limit if the degree of perturbation is set too large. To reduce this DLS limit risk the degree of perturbation can be limited, but that would restrict the freedom of movement of the well, potentially impacting the selection of the optimal trajectory. However, when spherical coordinates are used, movement of a well section is defined relative to the well section before it. The same reference point for the spherical coordinate system is used for every well section. A graphical representation of this phenomenon is displayed in Fig. 5. Having more freedom to move per iteration, without reaching the DLS limit, gives the method a higher probability of entering a neighboring domain of attraction and or achieving an optimum in fewer iterations. It must be noted that this issue can also be solved by smoothing the well trajectory as a post-processing step staying within DLS constraints (Vlemmix et al. 2009).
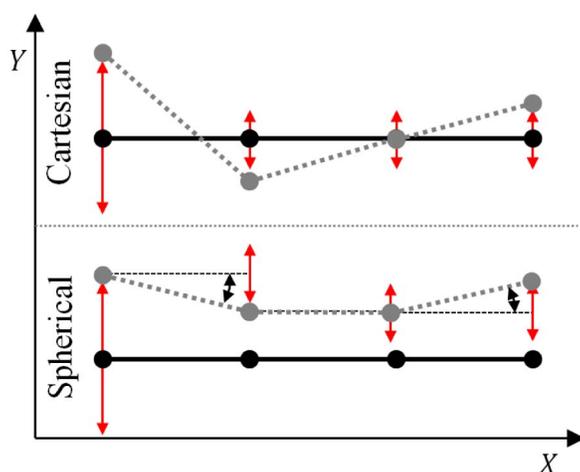
Figure 5—An *x-y* **view of two well trajectories, one using Cartesian coordinates (top) and one using spherical coordinates (bottom). Both were constructed using the same initial trajectory and outcome of Cz_i. It can be seen that the top trajectory probably does not stay within the DLS limit, but the bottom one does.**

Well Within Reservoir

The reason that the well has to lie within the reservoir is because the optimization algorithm is shown to perform significantly better than without the constraint. This was important due to the limited number of concurrent runs that were possible on the machine that was used in this study. When all the ensemble

members lie fully or partly outside of the reservoir it takes the algorithm longer to locate an optimum. The reason for this is that when a section of the well is not connected to the grid of the reservoir, it does not produce. This could result in a suboptimal trajectory. It is noted that an optimal well trajectory for a given reservoir does not necessarily lies completely within the reservoir. The constraint can be easily switched off to test the performance per individual case.

Evaluating whether or not a well lies within the reservoir can be done by either sending the well trajectory data to the simulator and checking the well intersection data, or by evaluating if the well is within the reservoir before sending it to the simulator. Since the simulator used in this paper had a relatively large latency between input and export of data, a pre-processing method was used to increase the algorithm's efficiency. The pre-processing method uses the corner point data of the top and bottom layer of the reservoir to determine if a node that describes the well trajectory lies within the reservoir. The method works in two consecutive steps. The first step is evaluating if the node lies in-between the x-y planes of the top and bottom layers. The second step is to evaluate if the node lies between the z planes of the top and bottom layer. A detailed explanation of this procedure can be found in Maas (2016).

Objective Function

The objective of the optimization discussed in this paper is to find a well trajectory that yields the highest NPV, and therefore the NPV will be used as the objective function. The NPV used in this study is defined as:

$$J(\mathbf{u}) = \sum_{k=1}^{K} \frac{[(r_o \cdot q_{o,k}) + (r_w \cdot q_{w,k}) + (r_g \cdot q_{g,k})] \Delta t_k}{(1+d)^{\frac{t_k}{\tau_t}}} \tag{3}$$

where the vector $\mathbf{u}$ is the control vector, representing the well trajectory; q_o, q_w and q_g are the production rates for oil, water [bbl/d], and gas [MMscf/d] respectively; r_o, r_w and r_g are, if positive, the wellhead prices, if negative, the handling costs of oil [USD/bbl], water [USD/bbl], and gas [USD/MMscf] respectively; Δt_k is the difference between consecutive time steps in days; d is the discount rate; K is the number of time steps; t_k is the cumulative time in days corresponding to time step k; τ_t is the reference time period used for discounting; in this case 365.25 days.

There are several methods that can be used to calculate the NPV. In the method described above, the NPV is discounted per time step as used in the reservoir simulator. Although not used in this paper, standard practice in the NPV calculation of most hydrocarbon recovery projects is to calculate the discounting element using a time step of one year. Another commonly used method for NPV calculation in optimization procedures is the calculation of a continuous NPV throughout the time step.

To ensure a proper comparison between objective functions of different simulations so that only $\mathbf{u}$ has influence on the NPV, two factors have to be taken into account. Firstly, a different time step size can alter the outcome of the simulation. Secondly if $d > 0$, the time steps have an influence on the discounting element of the NPV calculation. If the time steps differ between simulations, it could result in NPV changes due to the discounting element instead of $\mathbf{u}$. There are two ways to counteract these problems, the first is to fix the time step for each simulation, e.g. to 10 days. The second option is to interpolate the production data into fixed steps or to discount using one year time steps. Although this does not solve the first issue, it can mitigate a large part of the error caused by the discounting element.

In this study the reservoir simulator has been given a maximum time step of 20 days and the production data is interpolated into fixed intervals.

Smart Completion

In this section the completion that was used as the smart completion is discussed. The choice has been made to use an autonomous valve instead of a valve that has to be operated (e.g. an ICV). The reason for this

was to simplify the optimization method so no active open/close strategy was needed in the method. In this research the relatively new inflow control valve, AICV (InflowControl 2016), was used as the smart completion. The valve combines the main advantages of an AICD and ICV (Aakre et al. 2013, 2014). Like an AICD the valve is self-regulating and does not require any connection to the surface. The advantage of an AICV over an AICD is that it can shut off unwanted gas and water production completely. The AICV is also reversible, which means that a closed valve can autonomously open itself once it detects oil again.

The reservoir simulator that was used did not have the option to model AICVs directly, but did have the ability to model ICVs. Using the AICV's closing sequence as described in Aakre et al. (2014), the ICVs were coded within the simulator in such a way that they mimicked the AICVs. For the smart well completion, every well section comprised a tubing packer and an ICV. The configuration of the completion can be seen in a schematic cross section of the well in Fig. 6. To further optimize the smart well completion, the closing sequence of the ICVs, the location and amount of the ICV and packers need to be optimized as well. This was out of the scope of this research.
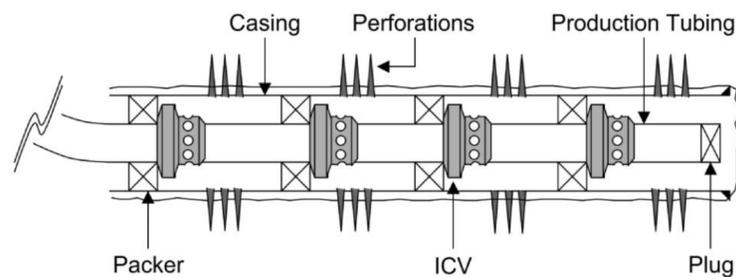

Figure 6—A schematic overview of the smart well configuration, which consist of tubing, packers and ICVs. (Naus et al. 2006)

Case Studies

To assess the algorithms, both were tested on a sector model of a reservoir. In this section the model and the results of both optimization methods are discussed. The name and the location of the reservoir are not given for confidentially reasons.

Reservoir Model

The sector model used, was a three-dimensional model of a plunging anticline dipping in both east and west directions. A 3D view of the model can be seen in Fig. 7.
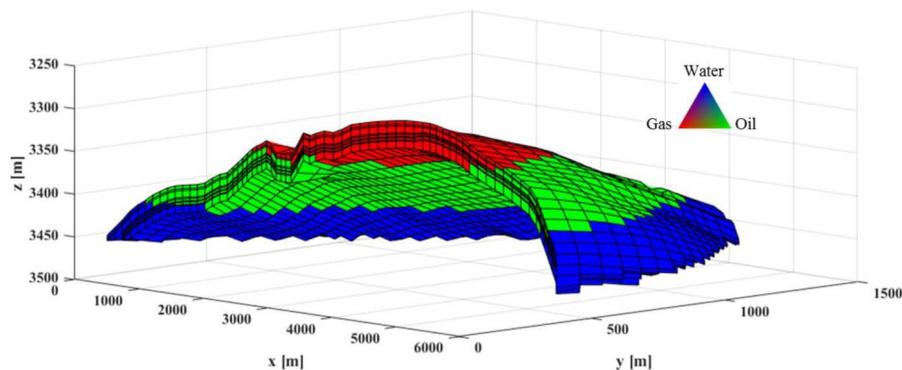

Figure 7—A 3D view of the reservoir model. The z scale in the plot is scaled, so the dip and the layering of the reservoir is more clearly visible.

The model, which is similar to the one used by Vlemmix et al. (2009), consist of in total 10800 (x:80, y:15, z:9) grid blocks of which 6621 are active. The dimensions of the reservoir are 5.50 km in the x direction,

1.34 km in the y direction and 192 m in the z direction. The latter is the vertical distance between the highest and lowest part of the reservoir. The average thickness of the reservoir is approximately 30 m. As can be seen in Fig. 7, a gas cap overlays the oil layer, which, in turn, lies above an aquifer. In the figure oil is depicted in green, gas in red and water in blue. To model the aquifer, a pore volume multiplier of 2000 was applied to the grid blocks below the oil/water contact (OWC). The OWC is located at a depth of 3348 m and the gas/oil contact (GOC) at 3415 m. The reservoir is heterogeneous with permeabilities varying between 6.5 mD and 2627 mD. In Table I it can be seen that the horizontal permeabilities (k_x, k_y) are the same and the vertical permeability (k_v) is one tenth of the horizontal ones. Fig. 8 depicts a cross section of the reservoir where the k_x of the different layers are shown. Furthermore, a transmissibility multiplier of 0.2 was applied to a certain area of the reservoir so that part of the reservoir is expected to show a different development of water or gas production. In this setting, a smart completion should have a bigger impact on the NPV. Fig. 9 shows the part of the reservoir where the transmissibility multiplier is used. The multiplier is applied to all layers within the area marked in the figure.

Table I—Rock Properties

Symbol	Min-Max	Average	Unit
ϕ	0.09-0.28	0.25	[-]
k_x	65-2627	918	[mD]
k_y	65-2627	918	[mD]
k_v	6.5-262.7	91.8	[mD]

Table II—Fluid Properties at Standard Conditions

Symbol	Value	Unit
ρ_o	850	[kg/m^3]
ρ_w	1000	[kg/m^3]
ρ_g	0.7	[kg/m^3]

In the reservoir a black oil model is used with oil of 35 degrees API and an initial gas/oil ratio (GOR) of 500 scf/STB. More details on the fluid properties can be found in Table II. The following relative permeabilities (k_r) were used; $k_{rw} = 0.2$, $k_{ow} = 0.2$, $k_{rog} = 0.2$, $k_{rg} = 0.05$. All had end points of 1 and Corey exponents of 2.
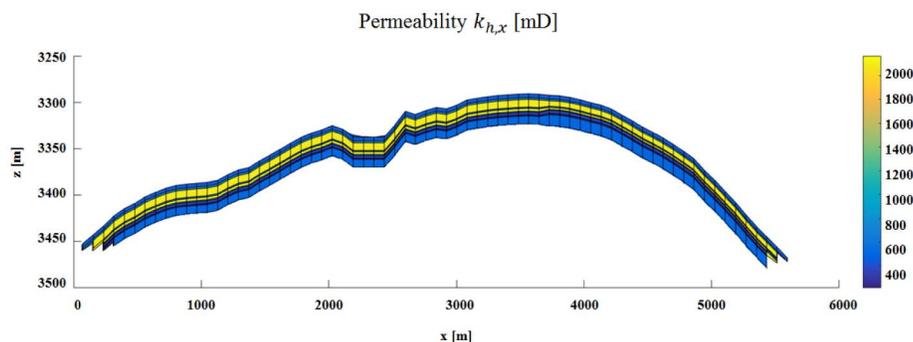

Figure 8—An x-z cross section of the reservoir, showing the permeability of the different layers. In the image, the zone with the transmissibility multiplier is not visible. The same stretched z scale is applied as in Fig. 7 to emphasize the layering.
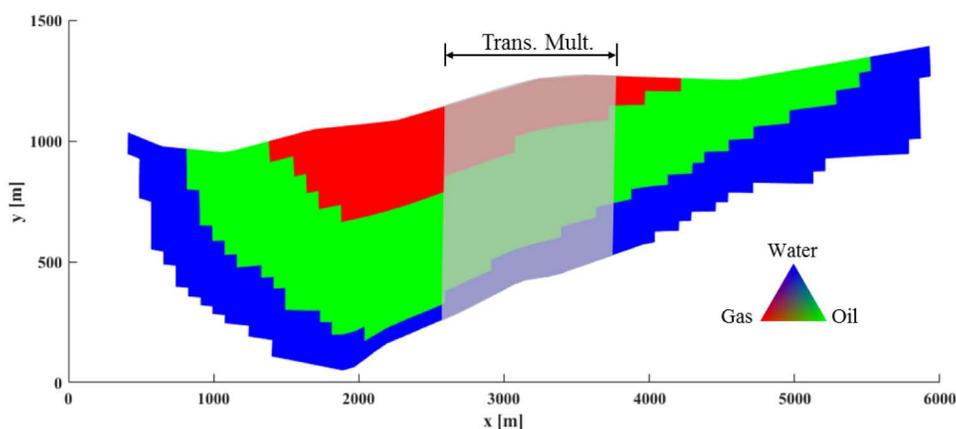
Figure 9—An *x-y* view of the reservoir model, with the transmissibility multiplier zone indicated.

Results

Conventional Completion

As discussed in the Introduction, first the optimal well trajectory for the conventional well has to be found, which can then be compared to the optimal trajectory of the smart well. To asses the optimum for the conventional completion first an initial well trajectory was chosen manually. The well was set as the initial control vector $\mathbf{u}^\ell$ and thus formed the starting point of the optimization procedure. In Fig. 10 the location of the initial well, which is depicted in red, can be seen. For simplicity reasons an open-hole completion was used for the conventional well. Both the SPS1 and SPS2 method were evaluated using the economic parameters listed in Table III.

Table III—Economic Parameters

Symbol	Value	Unit
r_o	40	[$/STB]
r_w	-10	[$/STB]
r_g	0	[$/Mscf]
d	10	[%/y]

In Table IV the input parameters of the SPS algorithm are shown. In this case a maximum number of iterations of 500 is taken. For the SPS1 method it is likely that the objective function would not change after these many iterations because it has probably converged before the 500th iteration. When using the SPS2 method a trade off has to be made between computation time and the likelihood that the algorithm can find a higher optimum when increasing the number of iterations. The well was divided into 10 sections to give the well the freedom to move trough the reservoir and to demonstrate how the optimization method would perform when dealing with a relatively high-dimensional optimization problem.

The reservoir simulator was set so that the simulation would terminate if it reached 3650 days or when the well would stop producing. Furthermore, the well was tubing head pressure constrained, without any constraints on gas, oil and water production.

Table IV—SPS Parameters

Parameter	Value	Unit
Max No. Iteration	500	[-]
Ensemble members	10	[-]
Well sections	10	[-]
DLS Limit	3	[°/30m]

In Fig. 11 the results of the objective function (NPV) are shown for the SPS1 and SPS2 algorithms. It can be seen that both methods were able to find an optimal well trajectory that yielded a significantly higher NPV than the initial well. Furthermore it can be seen that the SPS1 method has probably converged to a local optimum as the objective function did not change after about 80 iterations. The SPS2 method, as expected, did not converge, but was able to find a trajectory with a higher NPV. This confirmed what has been seen from the results of the Rastrigin function in Section 3.4. In addition to the initial well, the optimal well trajectory found by SPS1 and SPS2 can be seen in Fig. 10. The SPS2-optimized trajectory ended up, as expected, far away from the OWC and close to the GOC. No penalty (handling cost) was set on the gas production, and as a result all the gas from the gas cap that was produced increased the NPV because of the gas lift it provided. The gas cap was not strong enough to generate massive gas breakthrough.
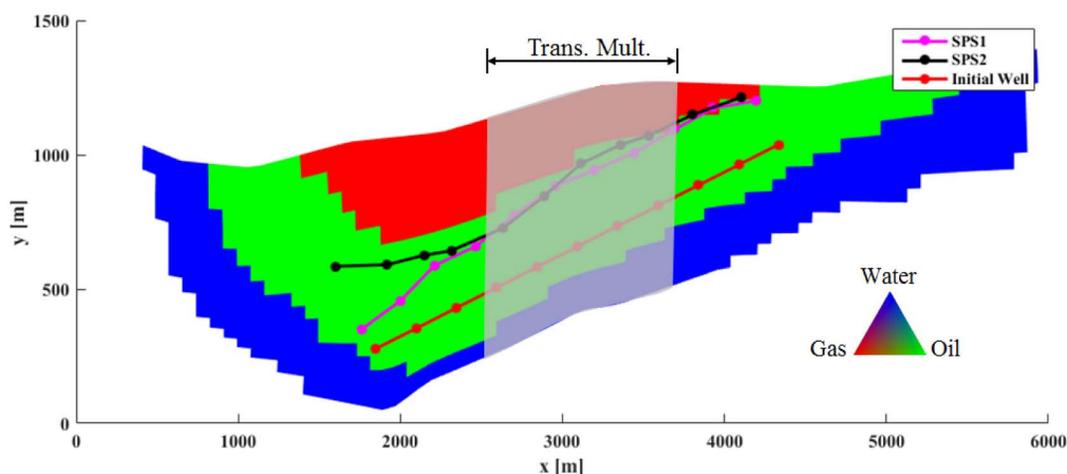

Figure 10—An *x-y* view of the reservoir showing the initial trajectory (red) and the optimal well trajectories as found by the SPS1 (magenta) and SPS2 (black) methods. All the wells in the figure have a conventional completion.
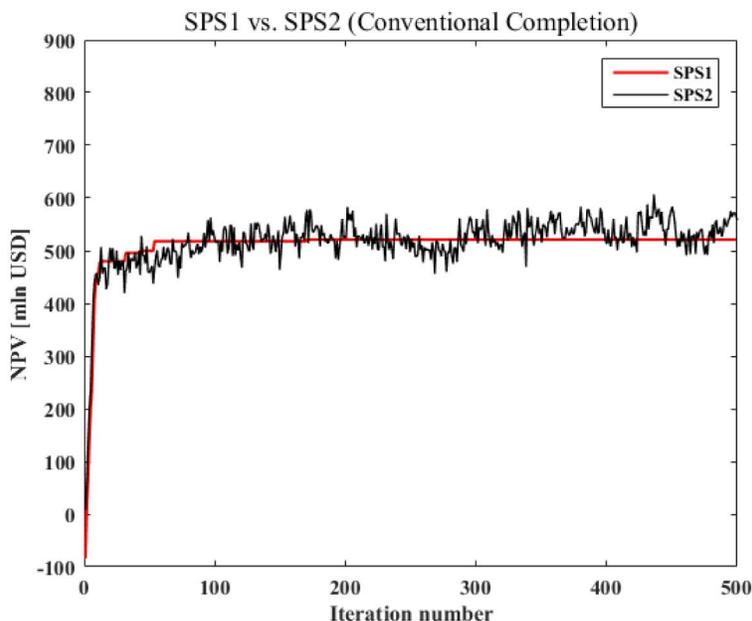
Figure 11—The objective function (NPV) results of the SPS1 (red) and SPS2 (black) methods for the conventional completion.

The production results of the initial and optimal (SPS2) trajectories are shown in Fig. 12. The production results from the initial well show that the well stopped producing before 3650 days were reached. This was a result of the well being unable to lift the fluids to surface due to the high water cut. The well found by SPS2 was able to produce for the full 3650 days and shows to have a lower water cut and higher oil and gas production, which resulted in a significantly higher NPV.
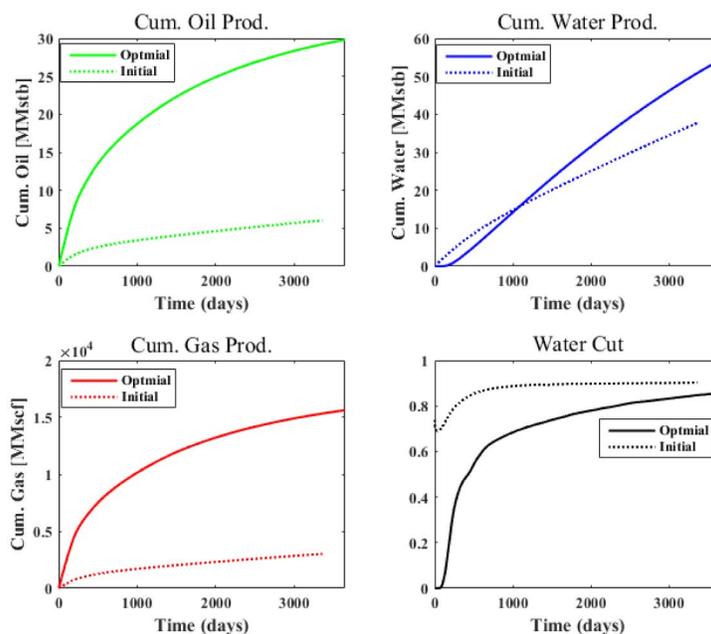

Figure 12—Plots of the production results of the optimal well (SPS2) and the initial well, both with conventional completions.

Smart Completion

Once the optimal well trajectory for the conventional completion had been found, it could be compared to that of the smart completion. This was done by setting the optimal conventional well trajectory found by SPS2 as the initial trajectory ($\mathbf{u}^\ell$) for the smart well trajectory optimization procedure. Both the SPS1

and the SPS2 method were evaluated. The algorithms, and the economic and SPS input parameters were identical to those used in the trajectory optimization of the conventional well. The plot in Fig. 13 shows that both SPS1 and SPS2 were able to find a well trajectory for the smart well completion that yields a higher NPV than the optimal trajectory that was found for the conventional completion. It can also be seen that SPS2, again, performs significantly better than SPS1. The NPV plot in Fig. 14 shows the comparison between the conventional and smart completion both optimized with the use of SPS2. From this plot it can be seen that the smart well completion does not yield a higher NPV if the trajectory is not optimized. The highest NPV value of the conventional completion is higher than the starting point of the smart completion.
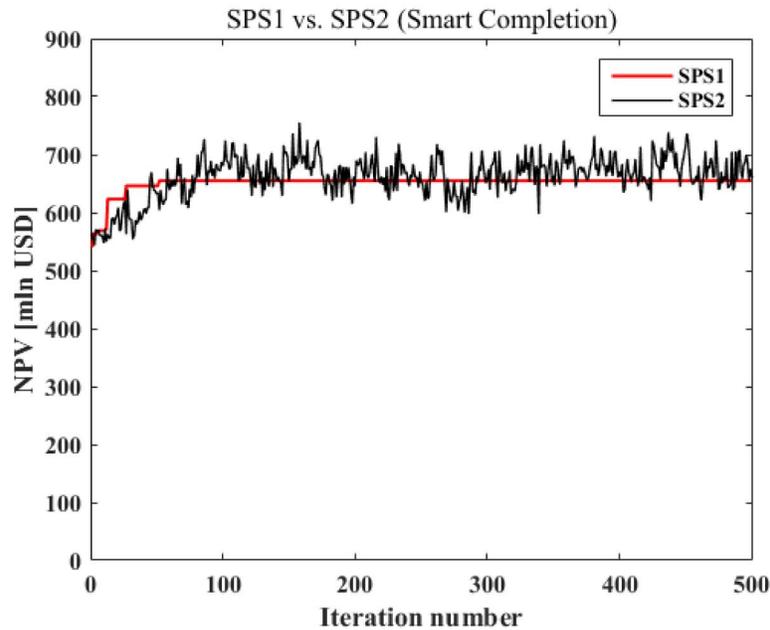
Figure 13—The objective function (NPV) results of the SPS1 (red) and SPS2 (black) method for the smart completion.
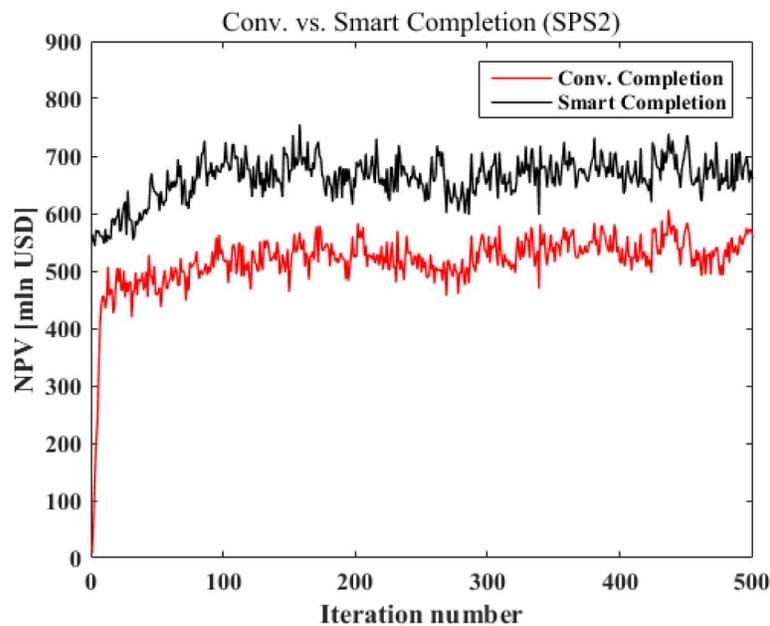
Figure 14—The objective function (NPV) results of the SPS2 (red) and SPS2 (black) method for the smart completion.

The difference between the two trajectories can be seen in Fig. 15. As expected, the trajectory of the smart well yields a higher NPV while it is closer to the OWC. The production results in Fig. 16 show that the smart well produces less oil than the conventional well, but also significantly less water, which contributes to a higher NPV. When the NPVs of the initial and optimized trajectory of the smart well are compared, a difference of 40% is observed. This implies that when smart completions are assessed, well trajectory optimization is crucial in evaluating the full potential of the completion. The plot in Fig. 14 also shows that the smart well has an NPV that is 25% higher than the NPV of the conventional well.
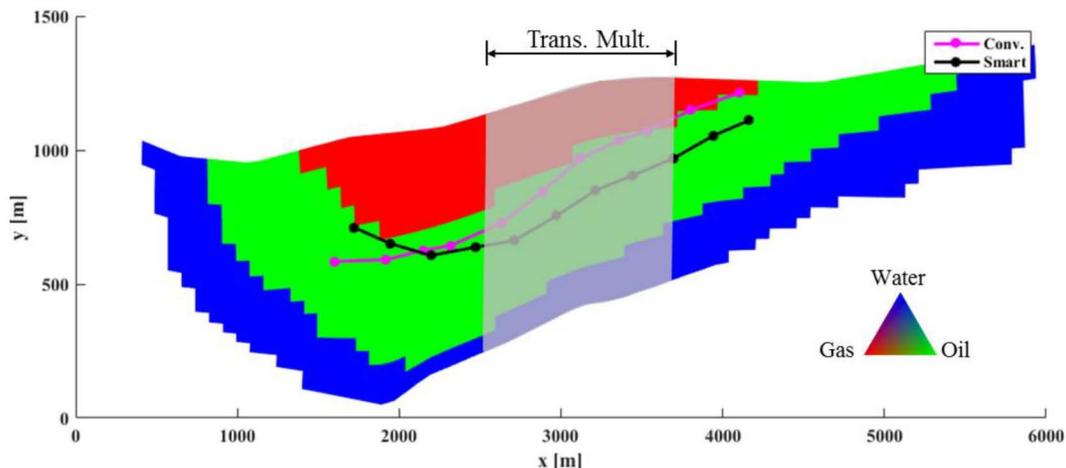

Figure 15—An *x-y* view of the reservoir showing the optimal conventional well trajectory (magenta) and the optimal smart well trajectory (black). Both trajectories were obtained using the SPS2 procedure.
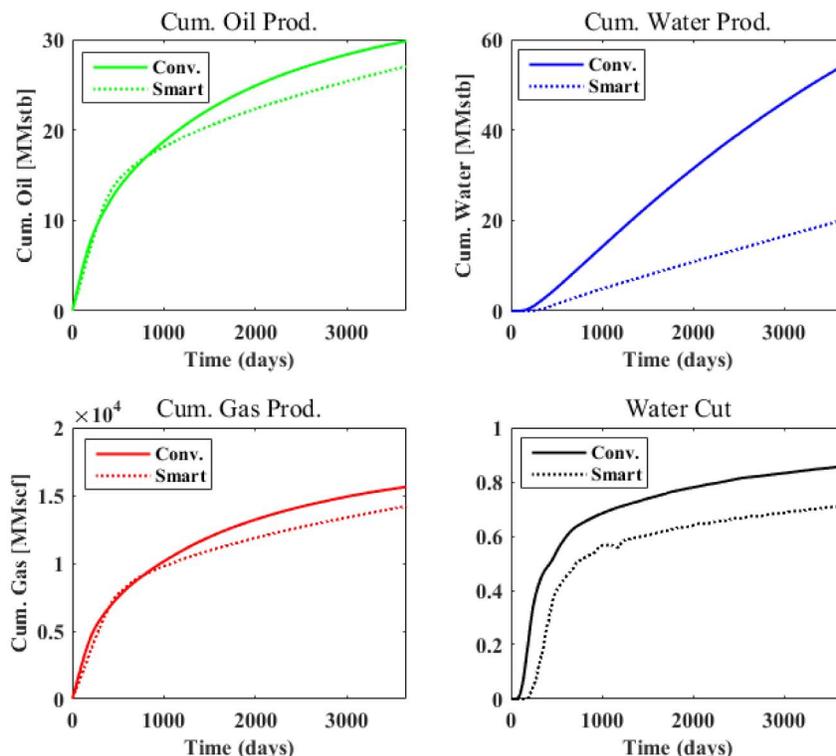

Figure 16—Plots of the production results of the optimal well (SPS2) with a conventional completion and the optimal well (SPS2) with smart completion.

Discussion, Recommendations and Conclusions

Discussion and Recommendations

- The reservoir model used in the case study had a relatively coarse grid. For the robustness of the algorithm, the modeling of the inflow of the well and coning effects, an overall finer grid or local grid refinement around the well is recommended. More research is needed to evaluate the trade off between computation time and the robustness of the method when refining the grid.

- No geological uncertainties (i.e. permeabilities, contacts etc.) were taken into account in the optimization methods. To assess the benefits of the smart well in a more robust manner, it is recommended to take these uncertainties into account. This can be done by including them into the optimization method as was done by Yeten (2003) or by separately running the algorithm on different reservoir realizations.

- In the NPV calculation no capital expenditures like completion costs and drilling cost were taken into account. To properly asses the economic benefits of any trajectory and any type of completion these have to be taken into account.

- To increase the algorithm's performance and decrease computation time, a constraint that the well trajectories had to lie fully within the reservoir was imposed. Because the optimal well trajectory does not necessarily have to lie fully within the reservoir, further study is needed on the performance of the algorithm without using this constraint when used on a machine where more concurrent runs are possible.

- The matrix $\mathbf{C}$ that limits perturbations of the control variables was tuned on a trial-and-error basis. Although the algorithm performed very well, further research on how to tune $\mathbf{C}$ is needed to optimize the method.

- The vector $\mathbf{z}$ was comprised of variables that were drawn from a univariate Gaussian distribution. Although it is not expected that the performance of the algorithm would significantly change if another distribution is used, research is needed to confirm this.

- The optimization of the closing sequence, sizes and locations of the smart completions were not evaluated in this research. Whether it is best to include these in the SPS method or optimize them with the use of another method needs to be investigated.

Conclusions

- The SPS1 and SPS2 methods both performed well when used to optimize a single well trajectory in a 3D reservoir. Although the SPS2 method, by design, does not converge, it performs significantly better than the SPS1 algorithm. This is because it has a higher probability to get out of local optima.

- By using the SPS methods it was shown that the optimal trajectory of a well with a conventional completion is not necessarily identical to the trajectory of the same well with a smart completion. Thus, when assessing the benefits of a well with smart completions it is recommended to optimize the well trajectory. Although no proof was given that the SPS2 method is the best method to do this, this research shows that, for the example considered, the use of the method is very effective even when only a small number of concurrent runs are possible.

- Because the SPS methods are not limited to the completion used in a well, they can be used for every completion type which does not have an active downhole inflow control ability. It is highly probable that every completion type has its own optimal well trajectory. The SPS methods provide an easy and quick way to evaluate this. When a well trajectory with active downhole inflow control is optimized, adding an additional optimization layer is recommended to optimize the control settings of the downhole valves.

- Although the SPS methods were only tested on one type of reservoir simulator it is believed that they are straightforward to implement in most commercial reservoir simulators.
- Because the SPS2 method has the feature that it has a high probability of evaluating different domains of attraction, it might provide a good benchmarking method for a wide range of optimization problems.

Nomenclature

List of Symbols

B = location of first node of well trajectory
C = perturbation matrix
d = discount rate
J = objective function [USD]
K = number of time steps
k = Permeability [mD]
K = iteration counter
L = well section length [m]
N = number of well sections
P = Pressure [Pa]
q = flow rate [oil/water: bbl/d][gas:MMscf/d]
r = price per unit volume [oil/water: USD/bbl][gas:USD/MMscf]
t = Time [d]
$\mathbf{u}$ = control variables vector
$\mathbf{z}$ = vector of random variables
β = dogleg angle [°]
θ = inclination
μ = viscosity
ρ = Density [kg/m³]
τ = reference period
φ = Azimuth [°]
Φ = porosity

Subscripts

g = gas
h = horizontal
k = time step counter
ℓ = iteration counter
o = oil
r = relative
w = water
v = vertical

Superscripts

T = transpose

Acronyms

AICD = Autonomous Inflow Control Device

AICV = Autonomous Inflow Control Valve
DLS   = Dogleg Severity
GOC   = Gas Oil Contact
GOR   = Gas Oil Ratio
ICD   = Inflow Control Devices
ICV   = Inflow Control Valves
NPV   = Net Present Value
MM   = Million
OWC   = Oil Water Contact
SCF   = Standard Cubic Feet
SPS   = Stochastic Pattern Search
STB   = Stock Tank Barrel

References

Aakre, H., Halvorsen, B., Werswick, B., & Mathiesen, V. 2013. Smart Well With Autonomous Inflow Control Valve Technology. Presented at the SPE Middle East Oil and Gas Show and Conference, Manama, Bahrain, 10-13 March. SPE-164348-MS. http://dx.doi.org/10.2118/164348-MS.

Aakre, H., Halvorsen, B., Werswick, B., & Mathiesen, V. 2014. Autonomous Inflow Control Valve for Heavy and Extra-Heavy Oil. Presented at the SPE Heavy and Extra Heavy Oil Conference: Latin America, Medellín, Colombia, 24-26 September. SPE-171141-MS. http://dx.doi.org/10.2118/171141-MS.

Addiego-Guevara, E., Jackson, M. D., & Giddins, M. A. 2008. Insurance Value of Intelligent Well TechnologyAgainst Reservoir Uncertainty. Presented at the SPE Symposium on Improved Oil Recovery, Tulsa, USA, 20-23 April. SPE-113918-MS. http://dx.doi.org/10.2118/113918-MS.

Afshari, S., Aminshahidy, B. and Pishvaie, M. R. 2011. Application of an improved harmony search algorithm in wellplacement optimization using streamline simulation. *Journal of Petroleum Science and Engineering* **78** (3-4) 664–678. http://dx.doi.org/10.1016/j.petrol.2011.08.009.

Alhuthali, A. H. H., Datta-Gupta, A., Yuen, B. B. W., & Fontanilla, J. P. 2009. Field Applications of Waterflood Optimization via Optimal Rate Control With Smart Wells. Presented at the SPE Reservoir Simulation Symposium, The Woodlands, USA, 2-4 February. SPE-118948-MS. http://dx.doi.org/10.2118/118948-MS.

Al-Khelaiwi, F. T. M. 2013. A comprehensive approach to the design of advanced well completions. Ph.D. dissertation, Heriot-Watt University.

Al-Khelaiwi, F. T. Birchenko, V. M. Konopczynski, M. R. and Davies, D. 2010. Advanced Wells: a Comprehensive Approach to the Selection Between Passive and Active Inflow-Control Completions. *SPEJ* **25** (3) 05–326. http://dx.doi.org/10.2118/132976-PA.

Bangerth, W., Klie, H., Wheeler, M. F., Stoffa, P. L., & Sen, M. K. 2006. On optimization algorithms for the reservoir oilwell placement problem. *Computational Geosciences* **10** (3), 303–319. http://dx.doi.org/10.1007/s10596-006-9025-7.

Bouzarkouna, Z., Ding, D. Y., & Auger, A. 2011. Well placement optimization with the covariance matrix adaptation evolution strategy and meta-models. *Computational Geosciences* **16** (1) 75–92. http://dx.doi.org/10.1007/s10596-011-9254-2.

Brouwer, D. R. and Jansen, J. D. 2004. Dynamic optimization of water flooding with smart wells using optimal control theory. *SPEJ* **9** (4) 391–402. http://dx.doi.org/10.2118/78278-PA.

Chen, Y. and Oliver, D. S. 2010:Ensemble-Based Closed-Loop Optimization Applied to Brugge Field. *SPEJ* **13** (1) 56–71. http://dx.doi.org/10.2118/118926-PA.

Chen, Y. 2008. Ensemble-Based Closed-Loop Production Optimization. Ph.D. dissertation. University of Oklahoma.

Dilib, F. A. Jackson, M. D. Zadeh, A. M. Aasheim, R., Årland, K., Gyllensten, A. J. and Erlandsen, S. M. 2015. Closed-Loop Feedback Control in Intelligent Wells: Application to a Heterogeneous, Thin Oil-Rim Reservoir in the North Sea. *SPEREE* **18** (1) 69–83. http://dx.doi.org/10.2118/159550-PA.

Do, S. T., & Reynolds, A. C. 2013. Theoretical connections between optimization algorithms based on an approximate gradient. *Computational Geosciences* **17** (6), 959–973. http://dx.doi.org/10.1007/s10596-013-9368-9.

Echeverrıa Ciaurri, D., Isebor, O. J. and Durlofsky, L. J. 2011a. Application of derivative-free methodologies to generally constrained oil production optimization problems. *International Journal for Mathematical Modeling and Numerical Optimization* **2** (2) 134–161. http://dx.doi.org/10.1504/IJMMNO.2011.039425.

Echeverrıa Ciaurri, D., Mukerji, T. and Durlofsky, L. J. 2011b. Derivative-Free Optimization for Oil Field Operations. In: *Computational Optimization and Applications in Engineering and Industry* 19–55. Eds. Yang, X. S. and Koziel, S., Springer. http://dx.doi.org/10.1007/978-3-642-20986-4_2.

Emerick, A. A. Silva, E., Messer, B., Almeida, L. F. Szwarcman, D., Pacheco, M. A. C. and Vellasco, M. M. B. R. 2009. Well Placement Optimization Using a Genetic Algorithm with Nonlinear Constraints. Presented at the SPE Reservoir Simulation Symposium, The Woodlands, USA, 2-4 February. SPE-118808-MS. http://dx.doi.org/10.2118/118808-MS.

Fonseca, R. M. Chen, B., Jansen, J. D. and Reynolds, A. C. 2017. A stochastic simplex approximate gradient (StoSAG) for optimization under uncertainty. *International Journal for Numerical Methods in Engineering* **109** (13) 1756–1776. http://dx.doi.org/10.1002/nme.5342.

Fonseca, R. M. Leeuwenburgh, O., Della Rossa, E., Van den Hof, P. M. J. and Jansen, J. D. 2015. Ensemble-Based Multi Objective Optimization of On-Off Control Devices Under Geological Uncertainty. *SPEREE* **18** (4) 1094–6470. http://dx.doi.org/10.2118/173268-PA.

Forouzanfar, F. and Reynolds, A. C. 2014. Joint optimization of number of wells, well locations and controls using a gradient based algorithm. *Chemical Engineering Research and Design* **92** (7) 1315–1328. http://dx.doi.org/10.1016/j.cherd.2013.11.006.

Forouzanfar, F., Poquioma, W. E. and Reynolds, A. C. 2016. Simultaneous and sequential estimation of optimal placement and controls of wells with a covariance matrix adaptation algorithm. *SPEJ* **21** (2) 501–521. http://dx.doi.org/10.2118/173256-PA.

Gai, H. 2001. Downhole Flow Control Optimization in the Worlds 1st Extended Reach Multilateral Well at Wytch Farm. Presented at the SPE/IADC Drilling Conference, Amsterdam, The Netherlands, 27 February-1 March. SPE-67728-MS. http://dx.doi.org/10.2118/67728-MS.

Gao, G., Vink, J. C., Alpak, F. O., & Mo, W. 2014. An Efficient Optimization Workflow for Field-Scale In-Situ Upgrading Developments. Presented at the Unconventional Resources Technology Conference, Denver, USA, 25-27 August. URTEC-2014–1885283. http://dx.doi.org/10.15530/URTEC-2014-1885283.

Grebenkin, I. M. 2013. A new optimisation procedure for uncertainty reduction by intelligent wells during field development planning. Ph.D. dissertation, Heriot-Watt University.

Güyagüler, B. and Horne, R. N. 2004. Uncertainty Assessment of Well-Placement Optimization. *SPEREE* **7** (1) 24–32. http://dx.doi.org/10.2118/87663-PA.

Güyagüler, B., Horne, R. N. Rogers, L. and Rosenzweig, J. J. 2002. Optimization of Well Placement in a Gulf of Mexico Waterflooding Project. *SPEREE* **5** (3) 229–236. http://dx.doi.org/10.2118/78266-PA.

Hart, W. E. 2001. A Convergence Analysis of Unconstrained and Bound Constrained Evolutionary Pattern Search. *Evolutionary Computation* **9** (1) 1–23. http://dx.doi.org/10.1162/10636560151075095.

Hooke, R. and Jeeves, T. A. 1961. 'Direct Search' Solution of Numerical and Statistical Problems. *Journal of the ACM* **8** (2) 212–229. http://dx.doi.org/10.1145/321062.321069.

Humphries, T. D. and Haynes, R. D. 2015. Joint optimization of well placement and control for nonconventional well types. *Journal of Petroleum Science and Engineering* **126** 242–253. http://dx.doi.org/10.1016/j.petrol.2014.12.016.

InflowControl. 2016. http://www.inflowcontrol.no/.

Isebor, O. J. Durlofsky, L. J. and Echeverría Ciaurri, D. 2014. A derivative-free methodology with local and global search for the constrained joint optimization of well locations and controls. *Computational Geosciences* **18** (3) 463–482. http://dx.doi.org/10.1007/s10596-013-9383-x.

Jansen, J. D. 2011. Adjoint-based optimization of multiphase flow through porous media – a review. *Computers and Fluids* **46** (1) 40–51. http://dx.doi.org/10.1016/j.compfluid.2010.09.039.

Jansen, J. D. Wagenvoort, A. M. Droppert, V. S. Daling, R., and Glandt, C. A. 2002. Smart well solutions for thin oil rims: Inflow switching and the smart stinger completion. Presented at the Asia Pacific Oil and Gas Conference and Exhibition, Melbourne, Australia, 8-10 October. SPE-77942-MS. http://dx.doi.org/10.2118/77942-MS.

Lee, J. W. Park, C., Kang, J. M. and Jeong, C. K. 2009. Horizontal Well Design Incorporated with Interwell Interference, Drilling Location, and Trajectory for the Recovery Optimization. Presented at the SPE/EAGE Reservoir Characterization and Simulation Conference, Abu Dhabi, UAE, 19-21 October. 125539-MS. http://dx.doi.org/10.2118/125539-MS.

Loomba, A. K. 2015. Well trajectory optimization. M.Sc. thesis. Delft University of Technology. uuid:897b5abe-0713-4c4a-ad5d-6c76d33c8bd2

Maas, T. R. 2016. Impact of Smart Completions on Optimal Well Trajectories. M.Sc. thesis. Delft University of Technology. uuid:834a71fe-3658-42c8-875e-bfd01192de7d

Molga, M., Smutnicki C. 2005. Test functions for optimization needs. http://www.zsd.ict.pwr.wroc.pl/files/docs/functions.pdf.

Naus, M. M. J. J., Dolle, N. and Jansen, J. D. 2006. Optimisation of Commingled Production Using Infinitely Variable Inflow Control Valves. *SPEPO* **21** (2) 293–301. SPE-90959-PA. http://dx.doi.org/10.2118/90959-PA.

Owunalu, J. E. and Durlofsky, L. 2010. Application of a particle swarm optimization algorithm for determining optimum well location and type. *Computational Geosciences* **14** (1) 183–198. http://dx.doi.org/10.1007/s10596-009-9142-1.

Petex. 2015. Reveal Reservoir Simulator. http://www.petex.com/products/?ssi=8/.

Pinto, M. A. S. Barreto, C. E. A. G., & Schiozer, D. J. 2012.Comparison Between Conventional and Intelligent Wells with Reactive and Proactive Controls under Economic Uncertainty. Presented at the SPE International Production and Operations Conference & Exhibition, Doha, Qatar, 14-16 May. SPE-155657-MS. http://dx.doi.org/10.2118/155657-MS.

Sarma, P. and Chen, W. H. 2008. Efficient Well Placement Optimization with Gradient-Based Algorithms and Adjoint Models. Presented at the SPE Intelligent Energy Conference and Exhibition, Amsterdam, The Netherlands, 25-27 February. SPE-112257-MS. http://dx.doi.org/10.2118/112257-MS.

Sarma, P., Aziz, K. and Durlofsky, L. J. 2005. Implementation of adjoint solution for optimal control of smart wells. Presented at the SPE Reservoir Simulation Symposium, Houston, USA, 31 January – 2 February. SPE-92864-MS. http://dx.doi.org/10.2118/92864-MS.

Schiozer, D. J. and Silva, J. P. Q. G. 2009. Methodology to Compare Smart and Conventional Wells. Presented at the SPE Annual Technical Conference and Exhibition, New Orleans, USA, 4-7 October. SPE-124949-MS. http://dx.doi.org/10.2118/124949-MS.

Torczon, V. 1997. On the Convergence of Pattern Search Algorithms. *SIAM Journal on Optimization* **7** (1), 1–25. http://dx.doi.org/10.1137/s1052623493250780.

Van Essen, G. M. Jansen, J. D. Brouwer, D. R. Douma, S. G. Zandvliet, M. J. Rollett, K. I. and Harris, D. P. 2010. Optimization of Smart Wells in the St. Joseph Field. *SPEREE* **13** (4) 588–595. http://dx.doi.org/10.2118/123563-PA.

Vlemmix, S., Joosten, G. J. P. Brouwer, D. R. and Jansen, J. D. 2009. Adjoint-Based Well Trajectory Optimization. Presented at the SPE Europec/EAGE Annual Conference and Exhibition, Amsterdam, The Netherlands, 8–11 June. SPE-121891-MS. http://dx.doi.org/10.2118/121891-MS.

Yeten, B. 2003. Optimum deployment of nonconventional wells. Ph.D. dissertation. Stanford University.

Yeten, B., Durlofsky, L. J. and Aziz, K. 2003. Optimization of Nonconventional Well Type, Location and Trajectory. *SPEJ* **8** (3) 200–210. http://dx.doi.org/10.2118/86880-PA.

Zandvliet, M. J. Handels, M., Van Essen, G. M. Brouwer, D. R. and Jansen, J. D. 2008. Adjoint-Based Well Placement Optimization Under Production Constraints. *SPEJ* **13** (4) 392–399. http://dx.doi.org/10.2118/105797-PA.

Zhang, K., Li, G., Reynolds, A. C. Yao, J. and Zhang, L. 2010. Optimal well placement using an adjoint gradient. *Journal of Petroleum Science and Engineering* **73** (3-4) 220–226. http://dx.doi.org/10.1016/j.petrol.2010.07.002.